Analytica Chimica Acta 1043 (2018) 81–88

Contents lists available at ScienceDirect

Analytica Chimica Acta

journal homepage: www.elsevier.com/locate/aca

A universal DNAzyme-based bioluminescent sensor for label-free detection of biomolecules

Qinfeng Xu [b, 1], Yan Zhang [a, 1], Dongxue Xiang [a, 1], Chen-chen Li [a, 1], Chun-yang Zhang [a, *]

[a] College of Chemistry, Chemical Engineering and Materials Science, Collaborative Innovation Center of Functionalized Probes for Chemical Imaging in Universities of Shandong, Key Laboratory of Molecular and Nano Probes, Ministry of Education, Shandong Provincial Key Laboratory of Clean Production of Fine Chemicals, Shandong Normal University, Jinan, 250014, China
[b] College of Food and Biological Engineering, Shaanxi University of Science and Technology, Xi'an, 710021, China

HIGHLIGHTS

- We develop a universal DNAzyme-based bioluminescent sensor for label-free detection of various biomolecules.
- DNAzyme can cleave its substrate and release AMPs for the generation of self-illuminating light emission.
- This sensor does not require either external labels or the reporting reagents.
- This sensor can generate an enhanced bioluminescence signal with zero background.

GRAPHICAL ABSTRACT

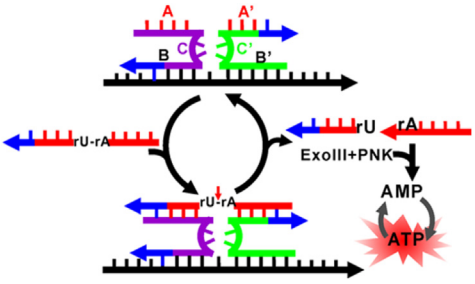

ARTICLE INFO

Article history:
Received 7 July 2018
Received in revised form
27 August 2018
Accepted 30 August 2018
Available online 31 August 2018

Keywords:
Biosensor
Bioluminescence
DNAzyme
DNA detection
Signal amplification

ABSTRACT

We demonstrate for the first time the development of a universal DNAzyme-based bioluminescent sensor for label-free detection of various biomolecules including DNAzyme and DNA. The presence of DNAzyme may induce the cyclic cleavage of riboadenosine (rA)-containing substrates, and the subsequent digestion of the cleaved substrates by exonuclease III (Exo III) releases abundant AMPs to initiate cyclic AMP pyrophosphorylation-ATP depyrophosphorylation for the generation of an enhanced bioluminescence signal. This sensor can real-time monitor the DNAzyme activity with a detection limit of 3.16×10^{-12} M. Moreover, the DNAzyme may be divided into two subunits for sensitive detection of target DNA. In the presence of target DNA, the two separated subunits may assemble into an active DNAzyme which can catalyze the cyclic cleavage of substrates and initiate the digestion of cleaved substrates by Exo III for the generation of an enhanced bioluminescence signal. This sensor can sensitively detect target DNA with a detection limit of 3.31×10^{-12} M. Importantly, this bioluminescent sensor can achieve a zero-background signal, and its output signal originates from the release of AMP for the generation of self-illuminating light emission without the requirement of either the external labels or the reporting reagents.

1. Introduction

DNAzymes are sequences of DNA with catalytic activity, and they are isolated via an in vitro selection technique [1]. DNAzymes are capable of catalyzing a broad range of chemical reactions such as RNA ligation, hydrolytic cleavage of DNA, phosphorylation, and

* Corresponding author.
E-mail address: cyzhang@sdnu.edu.cn (C.-y. Zhang).
[1] These authors contributed equally.

https://doi.org/10.1016/j.aca.2018.08.059
0003-2670/

deglycoslyation of RNA/DNA [2]. In comparison with ribozymes and proteins, DNAzymes are less expensive, easy synthetically prepared, more resistant to chemical and enzymatic degradation with the reduced nonspecific adsorption [1–3]. Biomedical research and clinical diagnosis call for highly sensitive bioanalytical platforms with the integration of signal amplification strategies. The DNAzyme-induced catalysis can be carried out with multiple turnovers and may introduce an amplification step into the bioanalytical platforms to achieve ultrahigh sensitivity [2–8].

DNAzyme as a biocatalyst has been used for the amplified detection of DNAs [4,9–12], metal ions [13–15], telomerase [16–18], and MTase activity [19,20]. Most of these DNAzyme-based methods employ fluorescent, colorimetric and chemiluminescent readout signals to indicate the presence of target biomolecules. However, the fluorescent assay [4,9,12,16] suffers from the complicated labeling of DNA probes with pair of fluorophores and quenchers, high background signal caused by external light excitation, incomplete quenching, and the intrinsic photofluorescence of biomolecules [21]. The colorimetric assay has the advantages of simplicity, low cost, and direct visualization with the naked eye, but it exhibits poor sensitivity and needs to avoid the optical absorption matrix of biological samples [10,13–15]. The peroxidase-mimicking DNAzyme-mediated chemiluminescent assay can provide much low intrinsic background emission, but it is time-consuming [11,18–20,22]. In contrast, the bioluminescent assay has distinct advantages of low background signal, high-throughput, self-illumination without the requirement for excitation, and especially its signal readout is less disturbed by autofluorescence, scattered light and photobleaching [23–25]. In this research, we develop a universal bioluminescent sensor for label-free detection of various biomolecules including 10–23 RNA-cleaving DNAzyme and DNA. The RNA-cleaving DNAzymes are a class of catalytic DNA molecules with excellent catalytic rates and turnover numbers as well as the capability to cleave a wide range of RNA substrate sequences [26,27]. Especially, the 10–23 RNA-cleaving DNAzymes have minimal size and can catalyze the cleavage of any purine-pyrimidine (RY) junction with high activity and specificity under a variety of conditions [28]. In this research, DNAzyme can catalyze the cleavage of an adenosine ribonucleotide (rA)-containing substrate, initiating the Exo III-induced digestion of the cleaved substrate and the subsequent release of AMP for the generation of an enhanced bioluminescence signal. In the proposed method, the output signal originates from the release of AMP for the generation of self-illuminating light emission without the requirement of either the external labels or the reporting reagents, and it can achieve zero-background signal. The bioluminescent sensor can real-time monitor the 10–23 RNA-cleaving DNAzyme activity with a detection limit of as low as 3.16×10^{-12} M, and it can sensitively detect target DNA with a detection limit of as low as 3.31×10^{-12} M. Importantly, it can be further applied to detect different target DNAs by simply changing the sensor arms of DNAzyme.

2. Materials and methods

2.1. Materials and reagents

All oligonucleotides (Table 1) were synthesized and HPLC purified by Sangon Biotechnology Co. Ltd. (Shanghai, China). The dCTP and DNA markers were purchased from Takara Biotechnology Co., Ltd. (Dalian, China). The exonuclease III (Exo III), T4 polynucleotide kinase (PNK) and 10 × Cutsmart buffer were obtained from New England Biolabs (Beverly, MA, USA). Phospho (enol)pyruvic acid monosodium salt hydrate (PEP), pyruvate kinase from rabbit muscle (PK), and adenylate kinase (AK) from rabbit muscle were purchased from Sigma-Aldrich, Inc. (St. Louis, MO, USA). The ATP determination kit was obtained from Invitrogen (Carlsbad, CA, USA). The 96-well white microplate and DEPC-treated water were purchased from Thermo Fisher Scientific (Pittsburgh, PA, USA). Ultrapure water was obtained from a Millipore filtration system.

2.2. Bioluminescent and gel electrophoresis analysis of RNA-Cleaving DNAzyme catalysis

All oligonucleotides were diluted with DEPC-treated water to prepare the stock solutions. The DNAzyme cleaving reaction was performed at room temperature for 1 h in 50 μL of reaction solution containing various-concentration 10–23 RNA-cleaving DNAzyme, 1×10^{-7} M substrate and 1 × Cutsmart buffer (50 mM potassium acetate, 20 mM tris-acetate, 10 mM magnesium acetate, 100 μg/mL BSA, pH 7.9, 25 °C). After incubation, the products were analyzed by bioluminescence measurement. For bioluminescence measurement, 50 μL of cleavage products was added into the ATP detection system with a final volume of 60 μL containing 10 U of Exo III, 3 U of PNK, 1 × Cutsmart buffer, 4.0 μL of AMP-to-ATP conversion buffer (1.0 μL of 1 U/μL AK, 1.0 μL of 1 U/μL PK, 1.0 μL of 10 mM dCTP, and 1.0 μL of 4.8 mM PEP), and 6 μL of ATP detection buffer (0.5 mM D-luciferin, 1.25 μg/mL firefly luciferase, 25 mM Tricine buffer (pH 7.8), 5 mM $MgSO_4$, 100 μM EDTA, and 1 mM DTT). The bioluminescence signal was measured with a Glomax 96-well luminometer (Promega, Madison, WI, USA) at room temperature. For gel electrophoresis, the DNAzyme cleaving reaction was performed at room temperature for 1 h in 10 μL of reaction solution containing 1×10^{-7} M 10–23 RNA-cleaving, 1×10^{-6} M substrate and 1 × Cutsmart buffer. Then DNAzyme cleaving products were analyzed by 12% nondenaturating polyacrylamide gel electrophoresis (PAGE) in 1 × TBE buffer (9 mM Tris-HCl, 9 mM boric acid, 0.2 mM EDTA, pH 7.9) at a 110 V constant voltage at room temperature for 40 min. The gel was stained with a silver staining kit (Tiandz Inc., Beijing, China).

2.3. Bioluminescent, fluorescent and gel electrophoresis analysis of target DNA

The reaction was performed at room temperature in 50 μL of reaction solution containing 1×10^{-7} M subunit (1), 1×10^{-7} M subunit (2), 1×10^{-7} M substrate, various-concentration target DNA and 1 × Cutsmart buffer (50 mM potassium acetate, 20 mM Tris-acetate, 10 mM magnesium acetate, 100 μg/mL BSA, pH 7.9) for 1 h at 25 °C, followed by bioluminescence measurement and gel electrophoresis described above. To validate the accuracy and precision of the proposed method, the fluorescence measurements with the labeled substrate (Table 1) were performed and compared with the bioluminescence measurements.

3. Results and discussion

3.1. Principle of bioluminescence monitoring of RNA-cleaving DNAzyme activity

The principle of bioluminescence monitoring of 10–23 RNA-cleaving DNAzyme activity is illustrated in Scheme 1. The typical DNAzyme system consists of an enzyme strand and a substrate strand. Both the DNAzyme strand and the substrate strand are modified with phosphorothioate at 3′ end to prevent the nonspecific digestion of exonuclease III (Exo III) [29,30]. The DNA substrate strand is 22 nt and it contains a cleavage site with an adenosine ribonucleotide (rA) followed by an uracil ribonucleotide (rU). The 10–23 RNA-cleaving DNAzyme contains a catalytic core flanked by two substrate-recognition binding arms (10 nt left and 11 nt right) that can bind to the substrate specifically, and the catalytic core of

Table 1
Sequences of oligonucleotides [a]

Note	sequence (5′–3′)
substrate	AAG GTT TCC TCrA rUCC CTG GGC AT*T* T*
labeled substrate	AAG GTT T(F)CC TCrA rUCC CT(Q)G GGC AT*T* T*
10-23 DNAzyme	TGC CCA GGG AGG CTA GCT ACA ACG AGA GGA AAC C*T*T*
subunits (1)	TGC CCA GGG AGG CTA GCT TAG TAC ATC TAA TAT ACT* G*G*
subunits (2)	AAA ATG AAG ACA GGT CTT TGA CAA CGA GAG GAA ACC*T*T*
target DNA	CCA GTA TAT TAG ATG TAC TAC AAA GAC CTG TCT TCA

[a] The asterisks indicate the phosphorothioate modification. The rA and rU in the substrate denote adenosine ribonucleotide and uracil ribonucleotide. The F and Q in the T bases of the labeled substrate denote the label of FAM and BHQ, respectively.

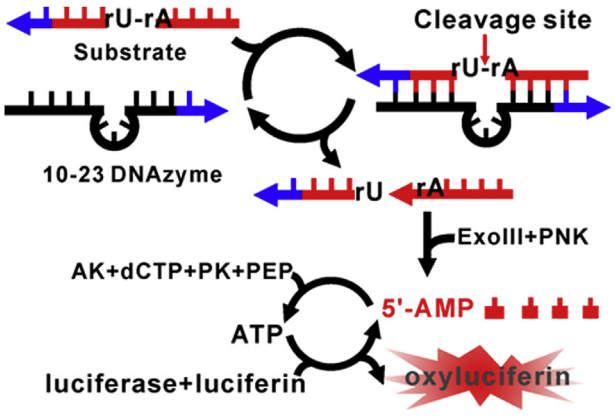

Scheme 1. Schematic illustration of bioluminescence monitoring of RNA-cleaving DNAzyme activity.

DNAzyme can cleave the scissile dinucleotide junction. In the presence of metal-ion cofactor (Mg^{2+}), the binding of the substrate to the 10–23 DNAzyme induces the hydrolytic cleavage of substrate at the scissile rArU dinucleotide junction. It should be noted that the 10–23 DNAzyme cleaves the RNA phosphodiester bond to yield a fragment with the 2′, 3′ cyclic phosphate group at the 3' end, which prevents the generation of AMP induced by Exo III digestion [31–33]. To solve this issue, T4 polynucleotide kinase (PNK) is introduced to remove the 2′, 3′ cyclic phosphate group, forming 2′ and 3′-hydroxyl termini [32]. Subsequently, the cleaved substrate with rA may be specifically degraded from its 3′-hydroxyl termini by Exo III to release a large number of deoxyribonucleotide monophosphates (including dAMP, dCMP, dGMP and dTMP), riboadenosine monophosphate (AMP) and DNAzyme strand. The reserved DNAzymes can further hybridize with new DNA substrates to initiate new cycles of cleavage-degradation-hybridization, generating abundant AMPs. The released AMP may be converted to ATP through the combination of the enzymatic reactions of adenylate kinase (AK) and pyruvate kinase (PK) in the presence of PEP and dCTP, and the subsequent conversion of ATP to AMP produces a distinct bioluminescence signal with the assistance of firefly luciferase and luciferin [34–36], enabling the real-time bioluminescence monitoring of RNA-cleaving DNAzyme activity. Notably, the released AMP may induce the cyclic AMP pyrophosphorylation-ATP depyrophosphorylation, generating an enhanced bioluminescence signal [37]. Unlike the fluorescent assay, the bioluminescent assay does not require an excitation light source to produce light emission, resulting in a near-zero background signal and consequently high sensitivity [23–25].

3.2. Feasibility of the DNAzyme-catalyzed substrate cleavage assay

To verify the DNAzyme-catalyzed cleavage of substrate, we used the denaturing polyacrylamide gel electrophoresis (PAGE) to analyze the cleavage products. In the presence of both DNAzyme and substrate, a new band of cleavage products is observed as a result of cleavage reaction. However, the band of the cleaved DNA is not observed in the presence of either substrate (Fig. 1A, lane 1) or 10–23 DNAzyme (Fig. 1A, lane 2), suggesting no occurrence of cleavage event. We further performed bioluminescence measurement to monitor the cleavage byproduct AMP induced by Exo III digestion. A near-zero background signal is observed in the presence of either DNAzyme (Fig. 1B, blue line) or the substrate (Fig. 1B, black line). In contrast, an enhanced bioluminescence signal is observed in the presence of both DNAzyme and substrate (Fig. 1B, red line), indicating that only the hydrolytic cleavage of substrate by DNAzyme can induce the Exo III digestion-mediated release of AMP for the production of a distinct bioluminescence signal through the enzymatic conversion of AMP to ATP.

3.3. Optimization of experimental conditions

Exo III is a double-stranded DNA (dsDNA)-specific nuclease and it can also digest the 3′-end of single-stranded DNA (ssDNA) as well [29,38]. Moreover, Exo III can efficiently degrade the RNA strand in DNA-RNA hybrids to release 5′-AMP [35,39]. To obtain the best performance, we performed the bioluminescent monitoring of the degradation of the cleaved substrate by Exo III and Exo III + PNK, respectively. As shown in Fig. 2A, in the presence of only Exo III, no significant bioluminescence signal is observed because 2′, 3′ cyclic phosphate group at the 3′ end after the cleavage of DNA substrate blocks the generation of AMP through the Exo III digestion [31–33]. In contrast, a high bioluminescence signal is observed in the presence of both Exo III + PNK, suggesting that the PNK can convert the 2′, 3′ cyclic phosphate group to 2′ and 3′-hydroxyl termini [32] and then Exo III can degrade the cleaved substrate to release 5′-AMP. Therefore, Exo III + PNK were used in subsequent experiments. In this assay, the bioluminescence signal relies on the digestion of Exo III, and thus the amount of Exo III should be optimized. We investigated the influence of Exo III upon the bioluminescence signal with a fixed amount of PNK (3 U). As shown in Fig. 2B, the bioluminescence signal enhances with the increasing amount of Exo III and reaches a plateau beyond the amount of 10 U. Therefore, 10 U of Exo III is used in the subsequent research.

3.4. Real-time bioluminescent monitoring of RNA-cleaving DNAzyme activity

Under the optimal conditions, we monitored the variance of bioluminescence in response to different-concentration RNA-cleaving DNAzyme in a real time. As shown in Fig. 3, the bioluminescence signal increases in both time-dependent and concentration-dependent manners. The higher the concentration of RNA-cleaving DNAzyme, the more the substrates being cleaved, consequently the more the released AMPs induced by Exo III

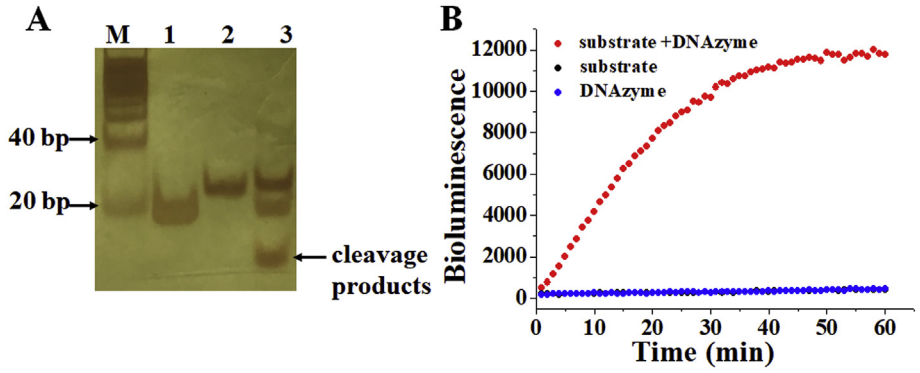

Fig. 1. (A) Gel electrophoresis analysis of RNA-cleaving DNAzyme. Lane M, DNA marker; lane 1, 1×10^{-6} M substrate; lane 2, 1×10^{-7} M 10–23 DNAzyme; lane 3, 1×10^{-7} M 10–23 DNAzyme $+1 \times 10^{-6}$ substrate. (B) Bioluminescence monitoring the byproduct AMP of DNAzyme-catalyzed cleavage reaction in the presence of 4×10^{-11} M 10–23 DNAzyme $+ 1 \times 10^{-7}$ M substrate (red line), 1×10^{-7} M substrate (black line), and 4×10^{-11} M 10–23 DNAzyme (blue line). (For interpretation of the references to color in this figure legend, the reader is referred to the Web version of this article.)

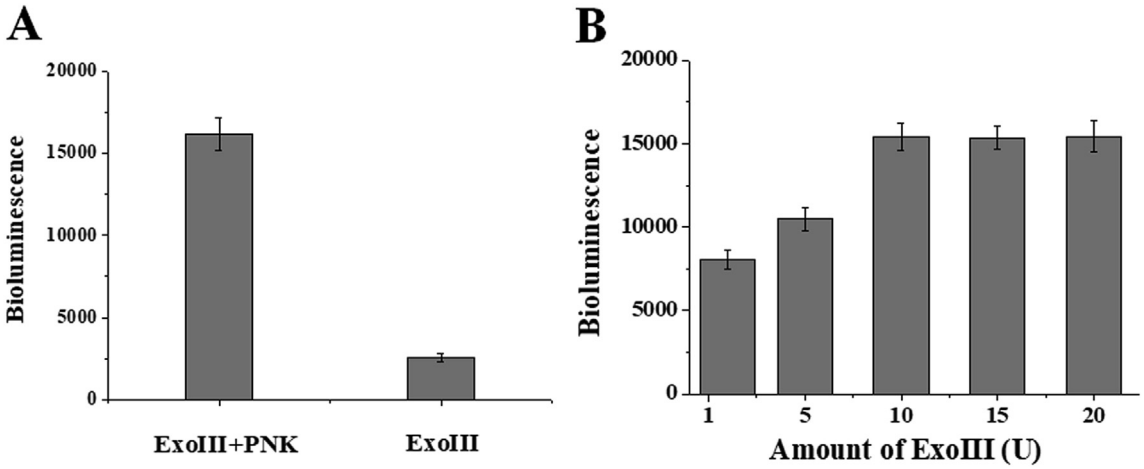

Fig. 2. (A) Bioluminescent monitoring of DNAzyme-catalyzed cleavage of substrate in response to different nucleases. The amount of Exo III is 10 U, and the amount of PNK is 3 U. (B) Bioluminescent monitoring of DNAzyme-catalyzed cleavage of substrate in response to different amount of Exo III at a fixed amount of PNK (3 U). Error bars show the standard deviations of three independent experiments.

digestion, and the higher the bioluminescence signal. In logarithmic scale, the bioluminescence intensity exhibits a linear correlation with the concentration of DNAzyme in a dynamic range of 3 orders of magnitude from 4×10^{-12} to 1×10^{-9} M (inset of Fig. 3). The regression equation is $B = 109781.18 + 9507.80 \log_{10} C$ ($R^2 = 0.9962$), where B is the bioluminescence intensity and C is the concentration of DNAzyme (M), respectively. The detection limit is calculated to be 3.16×10^{-12} M on the basis of the average signal of blank plus 3 times standard deviation. The improved sensitivity can be attributed to efficient signal amplification induced by 10–23 RNA-cleaving DNAzyme-catalyzed multiple turnover reactions and the recycling utilization of AMP. These results clearly demonstrate that bioluminescence monitoring of the released AMP can be used for RNA-cleaving DNAzyme assay.

3.5. Principle of target-triggered DNAzyme assembly-mediated DNA substrate cleavage for DNA detection

We further demonstrate the bioluminescence detection of target DNA based on target-triggered 10–23 RNA-cleaving DNAzyme assembly-mediated cyclic DNA substrate cleavage in combination with Exo III-assisted digestion of the cleaved substrate (Scheme 2). The 10–23 RNA-cleaving DNAzyme is split into subunits (1) and (2). The DNAzyme subunits (1) and (2) have multiple domains including substrate arms (domains A and A′) that bind to the substrate, partial catalytic core sequences (domains B and B′) that combine to provide a complete catalytic core upon assembly, and sensor arms (domains C and C′) that bind to target DNA. Both the subunits (1) and (2) are modified with phosphorothioate at the 3′ end to prevent the nonspecific digestion of Exo III [29,30]. The presence of target DNA and substrate initiates the cooperative assembly of active DNAzyme structure and subsequently the cleavage of substrate in the presence of Mg^{2+} ions to yield a fragment with the 2′, 3′ cyclic phosphate group at the 3′ end [31–33]. After the removal of 2′, 3′ cyclic phosphate group by PNK, the cleaved substrate fragment with free 3′ end can be specifically degraded by Exo III to release a large number of AMPs [32]. Notably, the assembled DNAzyme induced by target DNA can further hybridize with new DNA substrate to initiate new cycles of cleavage-degradation-hybridization, generating abundant AMPs and consequently an enhanced bioluminescence signal.

3.6. Feasibility of target-triggered DNAzyme assembly-mediated cyclic DNA substrate cleavage assay

To verify whether the target DNA-triggered DNAzyme can

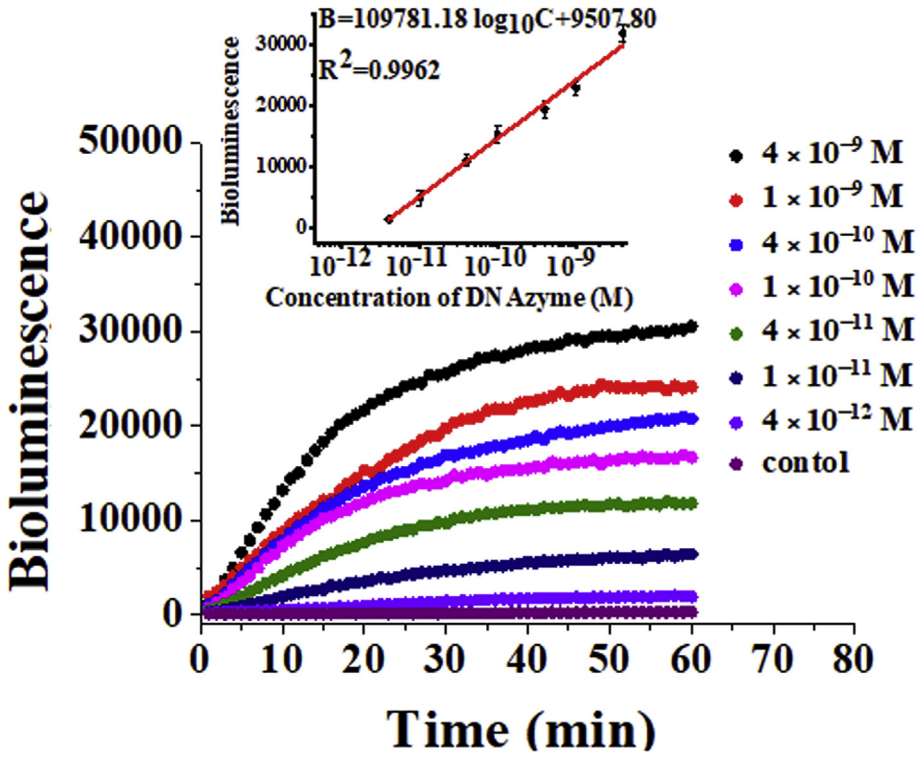

Fig. 3. Real-time monitoring of bioluminescence signal in response to different-concentration DNAzyme. Inset shows a linear correlation between the bioluminescence intensity and the logarithm of DNAzyme concentration in the range from 4×10^{-12} to 1×10^{-9} M. The bioluminescence intensities were obtained at 60 min. The substrate concentration is 1×10^{-7} M. Error bars show the standard deviation of three independent experiments.

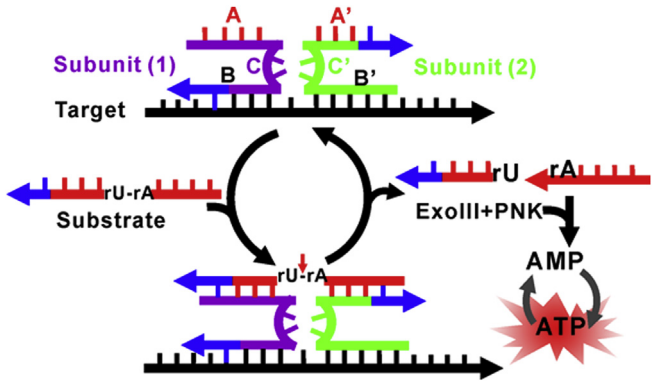

Scheme 2. Schematic illustration of DNA detection on the basis of target-triggered RNA-cleaving DNAzyme assembly-mediated cyclic DNA substrate cleavage.

cleave the substrate with similar fashion as the original DNAzyme, we performed the nondenaturating PAGE to analyze the reaction products. When the subunits (1) and (2) of DNAzyme, substrate and target DNA are present, a new band of the cleaved substrate fragment is observed (Fig. 4A, lane 7). In contrast, no cleaved substrate fragment is detected in the presence of substrate and the subunits (1) and (2) of DNAzyme without target DNA (Fig. 4A, lane 5). These results indicate that the binding of target DNA to the subunits (1) and (2) of DNAzyme can form an active DNAzyme structure to catalyze the substrate cleavage. We further performed the bioluminescence measurement to verify that target DNA can induce the formation of an active DNAzyme structure to catalyze the substrate cleavage. An enhanced bioluminescence signal is observed in the presence of subunits (1) and (2), target DNA and substrate (Fig. 4B, red line), with same bioluminescence enhancement being observed in response to the original DNAzyme (Fig. 1B, red line). While in the absence of subunits (1) and (2) (Fig. 4B, black line), target DNA (Fig. 4B, wine line), and substrate (Fig. 4B, blue line), no bioluminescence enhancement is observed with near-zero background signal (Fig. 4B). These results clearly demonstrate that target DNA can induce the formation of an active DNAzyme that can cleave the substrate to initiate Exo III-mediated digestion of the cleaved substrate for the generation of an enhanced bioluminescence signal.

3.7. Detection of target DNA

To investigate the sensitivity of the proposed method, we monitored the variance of bioluminescence signal in response to different-concentration target DNA. As shown in Fig. 5, the bioluminescence signal enhances with the increasing concentration of target DNA in a time-dependent manner. Moreover, the bioluminescence intensity exhibits a linear correlation with the logarithm of target DNA concentration in the range from 4×10^{-12} to 1×10^{-8} M (inset of Fig. 5). The regression equation is $B = 71944.65 + 6236.96 \log_{10} C$ with a correlation coefficient of 0.983, where B is the bioluminescence intensity and C is the concentration of target DNA (M). The detection limit is evaluated to be 3.31×10^{-12} M based on 3 times standard deviation over the blank response. The sensitivity of the proposed method has improved by 1 order of magnitude as compared with those of nicking endonuclease-assisted colorimetric assay (5×10^{-11} M) [40] and DNAzyme-gold nanoparticle-based colorimetric assay (5×10^{-11} M) [10], and is comparable to that of DNAzyme-based fluorescent assay (1×10^{-12} M) [4]. The improved sensitivity can be attributed to (1) the target DNA-triggered RNA-cleaving DNAzyme assembly-mediated cyclic DNA substrate cleavage, (2) the recycling utilization of AMP for the generation of an enhanced bioluminescence signal, and (3) the near-zero background signal

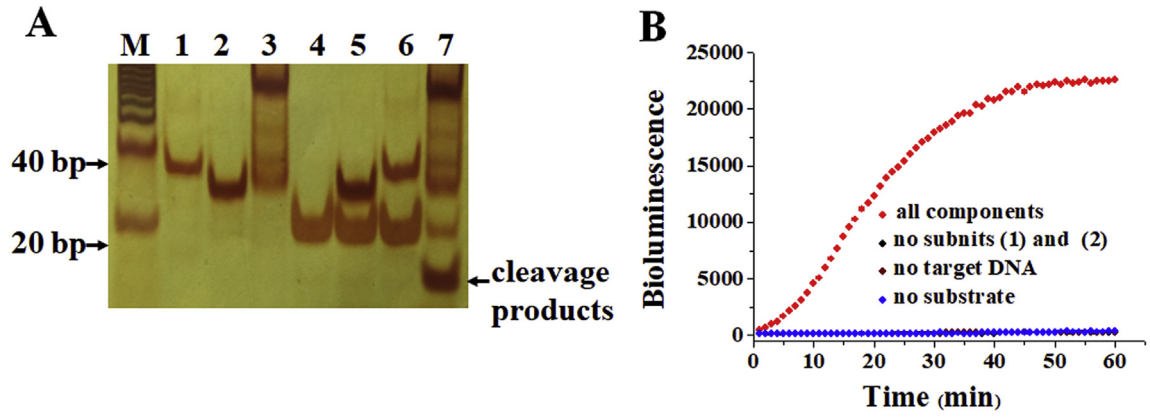

Fig. 4. (A) Gel electrophoresis analysis of the catalytic capability of target DNA-derived DNAzyme assembly. Lane M, DNA marker; lane 1, 1×10^{-7} M target DNA; lane 2, 1×10^{-7} M subunit (1) + 1×10^{-7} M subunit (2); lane 3, 1×10^{-7} M target DNA + 1×10^{-7} M subunit (1) + 1×10^{-7} M subunit (2); lane 4, 1×10^{-6} M substrate; lane 5, 1×10^{-6} M substrate + 1×10^{-7} M subunit (1) + 1×10^{-7} M subunit (2); lane 6, 1×10^{-7} M target DNA + 1×10^{-6} M substrate; lane 7, 1×10^{-6} M substrate + 1×10^{-7} M subunit (1) + 1×10^{-7} M subunit (2) + 1×10^{-7} M target DNA. (B) Bioluminescence monitoring of target DNA-triggered RNA-cleaving DNAzyme assembly-mediated DNA substrate cleavage. The 1×10^{-7} M subunit (1), 1×10^{-7} M subunit (2), 1×10^{-7} M substrate, and 4×10^{-9} M target DNA were used in the experiments.

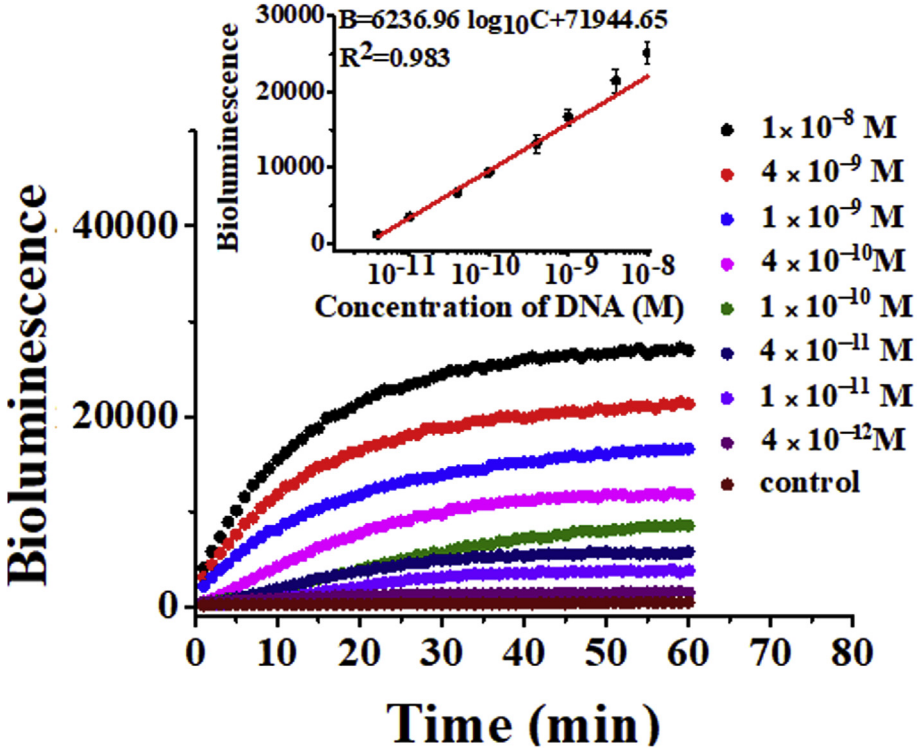

Fig. 5. Real-time monitoring of bioluminescence signal in response to different-concentration target DNA. Inset shows a linear correlation between the bioluminescence intensity and the logarithm of target DNA concentration in the range from 4×10^{-12} to 1×10^{-8} M. The bioluminescence intensities were obtained at 60 min. The 1×10^{-7} M subunit (1), 1×10^{-7} M subunit (2), and 1×10^{-7} M substrate were used in the experiments. Error bars represent the standard deviation of three independent experiments.

resulting from the self-illuminating light emission [23–25].

3.8. Real sample analysis

To demonstrate the feasibility of the proposed method for real sample analysis, we measured the target DNA spiked in fetal bovine serum (FBS). As shown in Fig. 6A, the bioluminescence signal enhances in a time-dependent manner in response to 1×10^{-10} M target DNA (Fig. 6A, red line) and 1×10^{-10} M target DNA in FBS (Fig. 6A, magenta line), while no significant bioluminescence enhancement is observed in the control groups with only pure buffer (Fig. 6A, black line) and FBS (Fig. 6A, blue line). The bioluminescence intensity in response to target DNA (Fig. 6B, red column) and target DNA in FBS (Fig. 6B, magenta column) are much higher than those obtained in the control groups with only FBS (Fig. 6B, blue column) and pure buffer (Fig. 6B, black column). Notably, a higher background signal is observed in response to FBS (Fig. 6B, blue column) than that in response to pure buffer (Fig. 6B, black column) due to the presence of a small amount of AMP, ADP, and ATP in FBS. The absolute concentration of target DNA in FBS is quantified to be 1.09×10^{-10} M with a recovery rate of 109%. These results demonstrate the high accuracy and good reproducibility of

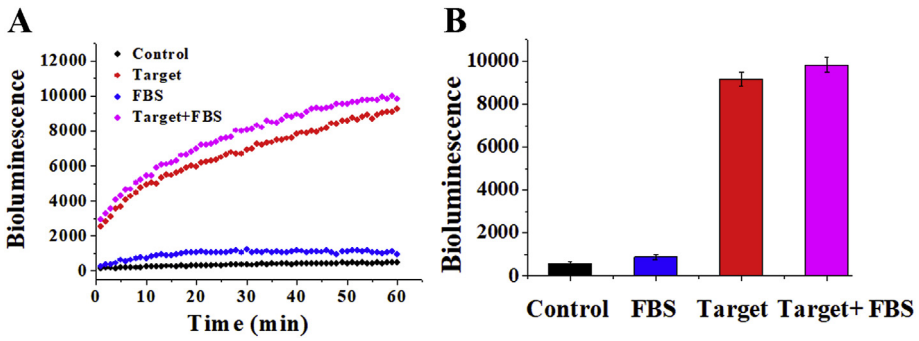

Fig. 6. (A) Real-time bioluminescence curves in response to target DNA + FBS (magenta line), target DNA (red line), FBS (blue line), and the control group with only pure buffer (black line). (B) Measurement of bioluminescence intensity in response to target DNA + FBS (magenta column), target DNA (red column), FBS (blue column), and the control group with only pure buffer (black column). The bioluminescence intensities in part B were obtained at 60 min. The target DNA concentration is 1×10^{-10} M. Error bars represent the standard deviation of three independent experiments. (For interpretation of the references to color in this figure legend, the reader is referred to the Web version of this article.)

the proposed method for real sample analysis. To further validate the accuracy of the proposed method, we compared our results with those obtained by the fluorescent measurement. Both the linear regression analysis and Bland–Altman analysis indicate no significant difference between our method and the fluorescent method (Fig. S1, see Supplementary Information). In addition, the coefficient of variation is 3.66% for the proposed method and 3.30% for the fluorescent method, indicating the good precision of the proposed method.

4. Conclusions

In summary, we have developed a universal bioluminescent sensor for label-free detection of various biomolecules including 10–23 RNA-cleaving DNAzyme and DNA. The 10–23 RNA cleaving DNAzyme can cleave a riboadenosine (rA)-containing substrate and initiate the Exo III-induced digestion of the cleaved substrate and the subsequent release of AMP for the generation of an enhanced bioluminescence signal. In comparison with the fluorescent assay [4,9,12,16], the output signal of the proposed method originates from the release of AMP for the generation of self-illuminating light emission without the requirement of either the external labels or the reporting reagents, and it can achieve a zero-background signal. Moreover, DNAzymes are less expensive, easy synthetically prepared, more resistant to chemical and enzymatic degradation with the reduced nonspecific adsorption. The DNAzyme may induce multiple turnovers catalysis of DNA substrate, and the released AMP can initiate cyclic AMP pyrophosphorylation-ATP depyrophosphorylation for the generation of an enhanced bioluminescence signal. This bioluminescent sensor can real-time monitor the 10–23 RNA-cleaving DNAzyme activity with a detection limit of 3.16×10^{-12} M, and it can sensitively detect target DNA with a detection limit of 3.31×10^{-12} M. Importantly, it can be further applied to detect different target DNAs by simply changing the sensor arms of DNAzyme.

Acknowledgments

This work was supported by the National Natural Science Foundation of China (Grant Nos. 21325523, 21527811, 21735003, and 21605098), the Award for Team Leader Program of Taishan Scholars of Shandong Province, China, and the Science and Technology Nova Plan of Shaanxi Province (2018KJXX-043), China.

Appendix A. Supplementary data

Supplementary data related to this article can be found at https://doi.org/10.1016/j.aca.2018.08.059.

References

[1] D.A. Baum, S.K. Silverman, Deoxyribozymes: useful DNA catalysts in vitro and in vivo, Cell. Mol. Life Sci. 65 (2008) 2156–2174.
[2] E. Mokany, S.M. Bone, P.E. Young, T.B. Doan, A.V. Todd, Mnazymes, a versatile new class of nucleic acid enzymes that can function as biosensors and molecular switches, J. Am. Chem. Soc. 132 (2010) 1051–1059.
[3] J.W. Liu, Z.H. Cao, Y. Lu, Functional nucleic acid sensors, Chem. Rev. 109 (2009) 1948–1998.
[4] F.A. Wang, J. Elbaz, C. Teller, I. Willner, Amplified detection of DNA through an autocatalytic and catabolic dnazyme-mediated process, Angew. Chem. Int. Ed. 50 (2011) 295–299.
[5] S. Sando, T. Sasaki, K. Kanatani, Y. Aoyama, Amplified nucleic acid sensing using programmed self-cleaving DNAzyme, J. Am. Chem. Soc. 125 (2003) 15720–15721.
[6] S.K. Silverman, Catalytic DNA (deoxyribozymes) for synthetic applications - current abilities and future prospects, Chem. Commun. (2008) 3467–3485.
[7] W.H. Zhou, J.S. Ding, J.W. Liu, Theranostic DNAzymes, Theranostics 7 (2017) 1010–1025.
[8] H.Y. Peng, A.M. Newbigging, Z.X. Wang, J. Tao, W.C. Deng, X.C. Le, H.Q. Zhang, DNAzyme-mediated assays for amplified detection of nucleic acids and proteins, Anal. Chem. 90 (2018) 190–207.
[9] F. Wang, J. Elbaz, R. Orbach, N. Magen, I. Willner, Amplified analysis of DNA by the autonomous assembly of polymers consisting of DNAzyme wires, J. Am. Chem. Soc. 133 (2011) 17149–17151.
[10] K. Zagorovsky, W.C.W. Chan, A plasmonic DNAzyme strategy for point-of-care genetic detection of infectious pathogens, Angew. Chem. Int. Ed. 52 (2013) 3168–3171.
[11] F. Wang, C.H. Lu, X.Q. Liu, L. Freage, I. Willner, Amplified and multiplexed detection of DNA using the dendritic rolling circle amplified synthesis of DNAzyme reporter units, Anal. Chem. 86 (2014) 1614–1621.
[12] C.H. Lu, F.A. Wang, I. Willner, Zn^{2+}-ligation DNAzyme-driven enzymatic and nonenzymatic cascades for the amplified detection of DNA, J. Am. Chem. Soc. 134 (2012) 10651–10658.
[13] J.W. Liu, Y. Lu, A colorimetric lead biosensor using DNAzyme-directed assembly of gold nanoparticles, J. Am. Chem. Soc. 125 (2003) 6642–6643.
[14] J.W. Liu, Y. Lu, Accelerated color change of gold nanoparticles assembled by DNAzymes for simple and fast colorimetric Pb^{2+} detection, J. Am. Chem. Soc. 126 (2004) 12298–12305.
[15] J.H. Lee, Z.D. Wang, J.W. Liu, Y. Lu, Highly sensitive and selective colorimetric sensors for uranyl (UO_2^{2+}) : development and comparison of labeled and label-free DNAzyme-gold nanoparticle systems, J. Am. Chem. Soc. 130 (2008) 14217–14226.
[16] Y. Zhang, L.J. Wang, C.Y. Zhang, Highly sensitive detection of telomerase using a telomere-triggered isothermal exponential amplification-based DNAzyme biosensor, Chem. Commun. 50 (2014) 1909–1911.
[17] V. Pavlov, Y. Xiao, R. Gill, A. Dishon, M. Kotler, I. Willner, Amplified chemiluminescence surface detection of DNA and telomerase activity using catalytic nucleic acid labels, Anal. Chem. 76 (2004) 2152–2156.
[18] T. Tian, S. Peng, H. Xiao, X.E. Zhang, S. Guo, S.R. Wang, X. Zhou, S.M. Liu, Highly sensitive detection of telomerase based on a DNAzyme strategy, Chem. Commun. 49 (2013) 2652–2654.
[19] W. Li, Z.L. Liu, H. Lin, Z. Nie, J.H. Chen, Label-free colorimetric assay for methyltransferase activity based on a novel methylation-responsive DNAzyme strategy, Anal. Chem. 82 (2010) 1935–1941.
[20] Y.P. Zeng, J. Hu, Y. Long, C.Y. Zhang, Sensitive detection of DNA methyltransferase using hairpin probe-based primer generation rolling circle amplification-induced chemiluminescence, Anal. Chem. 85 (2013)

6143–6150.
[21] K.A. Browne, D.D. Deheyn, G.A. El-Hiti, K. Smith, I. Weeks, Simultaneous quantification of multiple nucleic acid targets using chemiluminescent probes, J. Am. Chem. Soc. 133 (2011) 14637–14648.
[22] Y.J. Xu, D.D. Li, W. Cheng, R. Hu, Y. Sang, Y.B. Yin, S.J. Ding, H.X. Ju, Chemiluminescence imaging for microRNA detection based on cascade exponential isothermal amplification machinery, Anal. Chim. Acta 936 (2016) 229–235.
[23] A. Roda, M. Guardigli, E. Michelini, M. Mirasoli, P. Pasini, Analytical bioluminescence and chemiluminescence, Anal. Chem. 75 (2003) 462A–470A.
[24] Q.F. Xu, G.C. Zhu, C.Y. Zhang, Homogeneous bioluminescence detection of biomolecules using target-triggered hybridization chain reaction-mediated ligation without luciferase label, Anal. Chem. 85 (2013) 6915–6921.
[25] J. Inglese, R.L. Johnson, A. Simeonov, M.H. Xia, W. Zheng, C.P. Austin, D.S. Auld, High-throughput screening assays for the identification of chemical probes, Nat. Chem. Biol. 3 (2007) 466–479.
[26] S.K. Silverman, In vitro selection, characterization, and application of deoxyribozymes that cleave RNA, Nucleic Acids Res. 33 (2005) 6151–6163.
[27] M. Liu, D.R. Chang, Y.F. Li, Discovery and biosensing applications of diverse RNA-cleaving DNAzymes, Accounts Chem. Res. 50 (2017) 2273–2283.
[28] K. Schlosser, Y.F. Li, Biologically inspired synthetic enzymes made from DNA, Chem. Biol. 16 (2009) 311–322.
[29] Z.Y. Yang, A.M. Sismour, S.A. Benner, Nucleoside alpha-thiotriphosphates, polymerases and the exonuclease III analysis of oligonucleotides containing phosphorothioate linkages, Nucleic Acids Res. 35 (2007) 3118–3127.
[30] Y. Zhang, D.X. Xiang, B. Tang, C.Y. Zhang, Sensitive detection of transcription factor in nuclear extracts by target-actuated isothermal amplification-mediated fluorescence enhancement, Anal. Chem. 89 (2017) 10439–10445.
[31] S.W. Santoro, G.F. Joyce, A general purpose RNA-cleaving DNA enzyme, Proc. Natl. Acad. Sci. U.S.A. 94 (1997) 4262–4266.
[32] H. Schürer, K. Lang, J. Schuster, M. Mörl, A universal method to produce in vitro transcripts with homogeneous 3'- ends, Nucleic Acids Res. 30 (2002) e56-e56.
[33] Y.Y. Zhao, L. Zhou, Z. Tang, Cleavage-based signal amplification of RNA, Nat. Commun. 4 (2013) 1493.
[34] Q.F. Xu, S.Q. Huang, F. Ma, B. Tang, C.Y. Zhang, Controllable mismatched ligation for bioluminescence screening of known and unknown mutations, Anal. Chem. 88 (2016) 2431–2439.
[35] Q.F. Xu, F. Ma, S.Q. Huang, B. Tang, C.Y. Zhang, Nucleic acid amplification-free bioluminescent detection of microRNAs with high sensitivity and accuracy based on controlled target degradation, Anal. Chem. 89 (2017) 7077–7083.
[36] J. Du, Q.F. Xu, X.Q. Lu, C.Y. Zhang, A label-free bioluminescent sensor for real-time monitoring polynucleotide kinase activity, Anal. Chem. 86 (2014) 8481–8488.
[37] E.S. Burgos, S.A. Gulab, M.B. Cassera, V.L. Schramm, Luciferase-based assay for adenosine: application to s-adenosyl-l-homocysteine hydrolase, Anal. Chem. 84 (2012) 3593–3598.
[38] Q.F. Xu, A.P. Cao, L.F. Zhang, C.Y. Zhang, Rapid and label-free monitoring of exonuclease III-assisted target recycling amplification, Anal. Chem. 84 (2012) 10845–10851.
[39] R. Roychoudhury, R. Wu, Novel properties of Escherichia-coli exonuclease-III, J. Biol. Chem. 252 (1977) 4786–4789.
[40] W. Xu, X.J. Xue, T.H. Li, H.Q. Zeng, X.G. Liu, Ultrasensitive and selective colorimetric DNA detection by nicking endonuclease assisted nanoparticle amplification, Angew. Chem. Int. Ed. 48 (2009) 6849–6852.